U.S. CLIVAR
VARIATIONS
December 2008, Vol. 6, No. 3

Drought Reigns

by David M. Legler, Director

A recent workshop in Lincoln, Nebraska on Drought turned out to be a tremendously interesting and unprecedented gathering of the operational modeling and forecasting community (e.g. NCEP), those who develop routine/operational products and outlooks (e.g. NCEP, the National Drought Mitigation Center), and the research community who are helping to provide new insight and develop new capabilities. Working together and in harmony, these groups are mining for improved predictability of long-term drought, exploring the causes of drought, and discussing how best to improve the products and knowledge that can be conveyed through a suite of services.

This issue of Variations provides examples of some of the findings of the US CLIVAR Drought Working Group. The model runs the Working Group developed are now available for anyone to analyze, and since they are global runs, they are a potential source of new knowledge about drought in many regions of the world. Working Group members are preparing nearly ten manuscripts describing

Continued on Page Two

IN THIS ISSUE

Summer Drought and Heat Waves in Southern Africa: Observations and Coupled Model Behavior

Bradfield Lyon
International Research Institute for Climate and Society, Columbia University, NY, NY

During the severe summer drought of 1991-92 in southern Africa it is estimated that as much as 3 million tons of grain production were lost in this predominately rain-fed agricultural region (Dilley and Heyman 1995). The extreme high temperatures that accompanied the drought not only contributed to the crop losses but also to widespread livestock mortality (Sivakumar 2006) and stresses on regional water supplies (IPCC 2001). The joint occurrence of these two climate extremes is of consequence in any region of the globe although research has largely focused on the two phenomena considered in isolation. As part of the U.S. CLIVAR-led Drought in Coupled Models Project (DRiCOMP) a study was undertaken to examine how well climate models have performed in simulating the observed climate of the 20th Century with respect to generating drought, heat waves and their joint occurrence. The models were then utilized to assess, at least within (a subset of) coupled climate model space, how the concomitant occurrence of heat waves and drought may change under increasing anthropogenic forcing. The primary focus was on the subcontinent of southern Africa.

On monthly and seasonal time scales the tendency for summer rainfall and surface air temperature to be negatively correlated is of course well known with the physical linkage being via changes in the surface energy budget. Drier-than-average conditions reduce soil moisture favoring an increase in the surface sensible heat flux and thus higher surface air temperature. In southern Africa the tendency for below-average rainfall and above-average temperatures are often seen, for example, during El Niño events which tend to be associated with the near-synchronous occurrence of deficient rainfall and elevated surface air temperatures on the seasonal time scale (as in 1991-92). However, the relationship between shorter periods (i.e. several days) of extreme high temperatures (heat waves) and the occurrence of meteorological drought is less clear as daily maximum temperatures are also affected by variations in cloud cover, proximity to large water bodies, prevailing wind direction, thermal advection, etc. Indeed, for some coastal locations of southern Africa, this study finds that heat waves often occur in association with strong downslope flow generated by propagating synoptic weather systems which are distinct from the larger scale anomalous atmospheric circulation associated with drought (not shown).

The joint occurrence of heat waves and drought is also confounded by the prospect of climate change. For example, climate change scenarios are in general agreement that land surface temper-

Continued from Page One

their analysis indicating predictability of major SST patterns and trends, as well as soil moisture. Pegion and Kumar present one such effort in this issue. Another highlight of the Workshop was reviewing the findings of the Drought in Coupled Models (DRICOMP) funded research activities. They investigated mechanisms important for drought. Kerry Cook's paper in this issue focuses on the role of the Caribbean Low Level Jet in regional drought. U.S .CLIVAR's activities in drought are now ready to be documented and published. Watch for 13 manuscripts from DRICOMP PIs and others who attending the Drought Workshop, along with the Working Group manuscripts, that will be collected into a special issue of the Journal of Climate.

Drought-related research is not complete though. Much more could be done to understand the coupled ocean-atmosphere-land nature of drought and its forcings. Moreover, we don't fully know how well long-term drought can be predicted and we haven't yet fully considered how to develop early warning capabilities for drought and its evolution. There is no doubt drought research will remain critical for advancing our capabilities. Only by working with our colleagues in GEWEX, and with the operational and observations/products communities will we continue to make advancements that translate into improved products and services.

Variations

Published three times per year
U.S. CLIVAR Office
1717 Pennsylvania Ave., NW
Suite 250, Washington, DC 20006
(202) 419-3471
usco@usclivar.org

Staff: **Dr. David M. Legler**, *Editor*
Cathy Stephens,
Assistant Editor and Staff Writer

This newsletter is supported through contributions to the U.S. CLIVAR Office by NASA, NOAA—Climate Program Office, and NSF.

atures will increase in the 21st Century, generally increasing the probability of extreme daily temperatures (though not necessarily in a spatially uniform manner, e.g., Meehl and Tibaldi 2004). Yet these same models diverge considerably in their projected changes in precipitation, which in the case of southern Africa has some showing a drier, and others wetter, climate compared with the 20th century (IPCC 2007). Therefore, in the coming century there could potentially be more heat waves even in regions with upward trends in rainfall (even in the absence of drought), or decreased precipitation may lead to more frequent droughts, favoring the joint occurrence of heat waves via changes in surface heat fluxes.

The models utilized in the study were primarily the GFDL2.0, ECHAM5, and CSIRO3.5 all of which were included in the Coupled Model Intercomparison Project (CMIP-3), their output data archived at the Program for Climate Model Diagnosis and Intercomparison (PCMDI) website. For comparison with observations the 20th Century Climate in Coupled Model (20C3M) runs were utilized. Climate change projections were based on output from the same models forced with the A1B greenhouse gas scenario. The selection of the three models used here was based on their general ability to generate realistic ENSO characteristics (e.g., AchutaRao and Sperber 2006) while also having daily maximum surface air temperature (and other) data available for both the 20C3M and A1B runs. A heat wave was defined as a period of at least 3 consecutive days with the daily maximum surface air temperature (Tmax) exceeding the 90th percentile during the December–February season. The Tmax percentiles were obtained by ranking the daily data over the periods 1961-2000, 1981-2000, 2046-65 and 2081-2100. Drought conditions were based on different indicators including the three month Standardized Precipitation Index (SPI3), a related standardized drought index (WASP, Lyon and Barnston 2005), and one based on precipitation minus evaporation (P-E). Observational data included daily maximum temperatures for stations across South Africa for 1961-2000 and gridded monthly precipitation analyses obtained from the Global Precipitation Climatology Center (GPCC) for the same period.

The observational results are generally well-captured by the station analysis shown in Figure 1 for Kimberley, South Africa located in the central interior of the country (see Figure 2c). The unconditional probability (relative frequency of occurrence) of a heat wave occurring during any given month is 0.32. The probability of drought, defined as occurring when SPI3 is < -1.0, is 0.16. However, the conditional probability of a heat wave occurring given that drought conditions exist is 0.77 or about 2.4 times the unconditional probability (the conditional probability at Kimberley is greater than at several other stations, cf. Figure 2a, but in general it exceeds the unconditional prob-

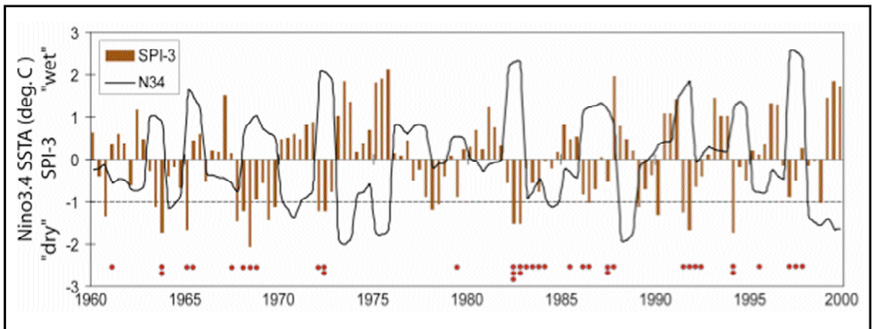

Figure 1. Times series of SPI3 (bars) and occurrence of heat waves (red dots) for individual months of the DJF seasons 1960-2000 at Kimberley, South Africa. The solid line represents the SST anomaly averaged over the Nino3.4 region. The correlation between Nino3.4 SST anomaly and SPI3 is -0.53. The Pr(Heat Wave) = 0.32; Pr(Drought SPI < -1) = 0.16, Pr(Heat Wave | Drought) = 0.77. The base period climatology used for both drought and heat waves is 1960-2000.

VARIATIONS

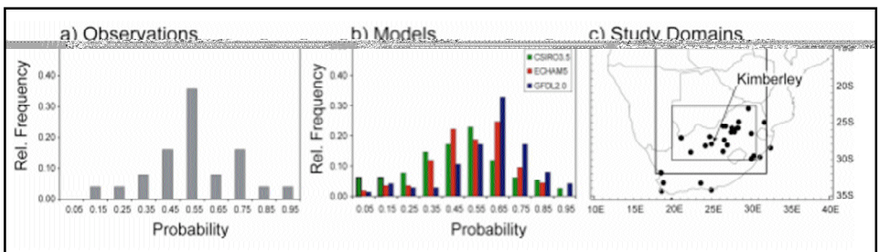

Figure 2. The relative frequency of occurrence of the conditional probability of a heat wave given drought conditions during the period 1960-200 based on a) station observations and b) coupled models (20C3M runs). Figure 3c shows the spatial domains used for the stations and models. The location of the Kimberley, South Africa station is shown by the arrow.

ability across most stations). The temporal correlation between SPI3 and the Nino 3.4 SST index is -0.53, indicating that El Niño (La Niña) events are often associated with drought (unusually wet) conditions. As such, the likelihood of a heat wave during an El Niño event is substantially enhanced relative to the unconditional probability while during La Niña it is markedly reduced. Figure 1 also indicates that there has been a clear increase in the number of heat waves at Kimberley during the past two decades.

The conditional probability of a heat wave given the existence of drought conditions was computed for all 21 stations located within the inner box shown in Figure 2c (station data was only available for South Africa), and across all model grid points in the larger, boxed domain (roughly 70-80 grid points depending on model) based on the 20C3M runs for the 1961-2000 period. The associated frequency distributions of the conditional probabilities are shown in Figures 2a and 2b, respectively. The observations and models show generally similar distributions with an enhanced likelihood of heat waves during drought relative to the unconditional probabilities, which (as seen for Kimberley) are typically around 0.3.

The joint occurrence of heat waves and drought for the models forced with the A1B greenhouse gas scenario is summarized in Figure 3a for model years 2046-65. A similar analysis was also performed for the model years 2081-2100 (not shown). Heat waves are based on Tmax percentiles obtained from the DJF seasons 2046-65. The drought index is also computed relative to this new base period climatology. The joint behavior (Figure 3a) does not show notably different behavior than for the observational period. However, relative to a 1981-2000 base period climatology the probability of a heat wave (Figure 3b) in the models shows a marked increase associated with a general upward trend in summer temperature in the models. Figure 3c shows that relative to the 1960-2000 base period drought conditions become more likely across much of southern Africa during 2046-65. This result, however, is highly model-dependent as can be seen by the dashed line in Figure 3c which indicates a tendency for wetter than average conditions when the analysis is based on output from the CRNM model. Indeed, there is not a consensus among all CMIP-3 models for drier conditions during summer in the coming century as suggested in the IPCC AR4 report. However, modeled droughts are generally exacerbated when surface evaporation is taken into account (i.e. using drought indices based on P-E, not shown) in the A1B runs.

Overall, the joint occurrence of heat waves and drought is generally similar in 20C3M runs and observations (conditional probabilities typically between 0.5 and 0.7 for both sets of data). While this behavior is similar in A1B runs when the two extremes are computed relative to future climate base states, from a practical viewpoint it is likely more meaningful to consider how they vary relative to the current climate. From the drought side, this includes consideration of changes in atmospheric demand for

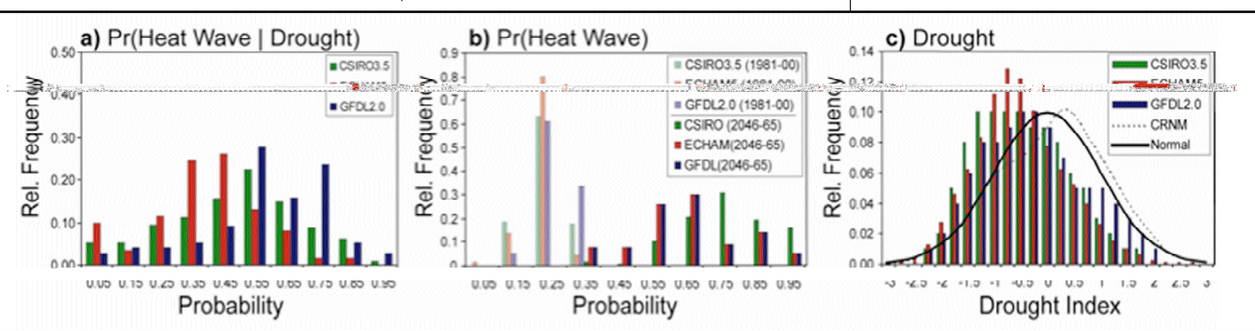

Figure 3. . a) The relative frequency of occurrence of the conditional probability of a heat wave given drought conditions computed from the model grid points within the larger domain in Figure 2c for model runs forced with the A1B greenhouse gases scenario. b) As in (a) but for the unconditional probability of a heat wave during the model years 1981-2000 (light shading) and 2046-65 (dark shading) using percentile rankings from 1981-2000. c) The relative frequency of drought index values for the model period 2046-65 using a 1960-2000 base period climatology. The solid line shows a normal distribution for the index and the dashed line is for the CRNM model.

water in a warmer climate. The full study is described in a manuscript currently being prepared for submission to the Journal of Climate.

Acknowledgements

This work was supported by a small grant for exploratory research from the National Science Foundation, NSF-ATM 07-39256. Daily maximum temperature data for stations across South Africa were kindly provided by the South African Weather Service. The comments of Tony Barnston on this work are also appreciated.

References

AchutaRao, K., and K.R. Sperber, 2006: ENSO simulation in coupled ocean-atmos - phere models: are the current models better? Clim. Dyn., 27, 1-15.

Dilley, M., and B.N. Heyman, 1995: ENSO and Disaster: Droughts, Floods and El Niño/Southern Oscillation Warm Events. Disasters, 19, 181-193.

IPCC, 2007: Climate Change 2007, The Physical Science Basis. Working Group I Contribution to the Fourth Assessment Report of the Intergovernmental Panel on Climate Change. Ch. 11. Cambridge University Press, NY, NY.

IPCC, 2001: Climate Change 2001: The Scientific Basis. Contribution of Working Group II to the Third Assessment Report of the Intergovernmental Panel on Climate Change [Houghton, J.T. et al., (eds.)]. Ch. 10.2.1.4. Cambridge University Press, United Kingdom and New York, NY.

Lyon, B., and A.G. Barnston, 2005: ENSO and the Spatial Extent of Interannual Precipitation Extremes in Tropical Land Areas. Journal of Climate, 18, 5095-5109.

Meehl, G.A., C. Tebaldi, 2004: More Intense, More Frequent, and Longer Lasting Heat Waves in the 21st Century. Science, 305, 994-997.

Sivakumar, M.V.K., 2006: Climate prediction and agriculture: current status and future challenges. Clim. Res., 33, 3-17. ■

Overview of the Drought Working Group Activities

Siegfried Schubert and David Gutzler, co-chairs

The U.S. CLIVAR Drought Working Group was established in November 2006 to "facilitate progress on the understanding and prediction of long-term (multi-year) drought over North America and other drought-prone regions of the world, including an assessment of the impact of global change on drought processes (Gutzler and Schubert 2007)". The specific tasks of the working group were to 1) propose a working definition of drought and related model predictands of drought, 2) coordinate evaluations of existing relevant model simulations, 3) suggest new experiments (coupled and uncoupled) designed to address outstanding uncertainties in the nature of drought, 4) coordinate and encourage the analysis of observational data sets to reveal antecedent linkages of multi-year droughts and 5) organize a community workshop to present and discuss the results.

This paper highlights the working group activities during its two-year tenure. While the working group has made progress on all five of the tasks listed above (the reader can for example find summaries and links to existing model simulations and relevant observational datasets at: http://www.usclivar.org/Organization/drought-wg.html), there are two areas that deserve particular attention. The first is the work done to develop drought indices of relevance to model prediction and evaluation. The second is the effort to design, coordinate and implement a new set of climate model simulations that address some of our key uncertainties about the role of sea surface temperature forcing and land-atmosphere feedbacks in the development and maintenance of drought.

The work on drought indices (Koster et al 2008), while acknowledging the historical importance of traditional indices such as the Palmer Drought Severity Index, focused attention on developing new indices that take advantage of information derived from land surface models and data assimilation techniques. The effort in particular addressed the robustness of soil moisture in the current generation of land surface models as an indicator of drought and more generally, hydro-climatic variability. This work provides a consistent assessment across models regarding drought prediction and simulation, and it supports the use of land surface models in drought monitoring activities.

The study took advantage of the GSWP-2 project (Dirmeyer et al. 2006) in which a number of land surface models were driven for 10 years with the same observations-based meteorological forcing. A key result of the study was the demonstration that, while the raw soil moisture output from the various models shows considerable differences, the results become much more similar after they are suitably normalized. The results are highlighted in Figure 1, which shows that the different land surface models produce very similar information about the temporal variability of soil moisture (and therefore drought) in many parts of the world when the soil moisture values from each model are normalized by their respective climatological means and variances. This indicates for example that one can use the current generation of Land Surface Models to reliably monitor drought in the United States Great Plains region.

The second major effort of the working group was the coordinated (multi-institutional and multi-model) development of a set of idealized simulations designed to improve our understanding of the physical mechanisms that link SST variations to regional drought, including an assessment of the role of land-atmosphere feedbacks (Schubert et al. 2009). Specific questions addressed by the experiments include: What are mecha-

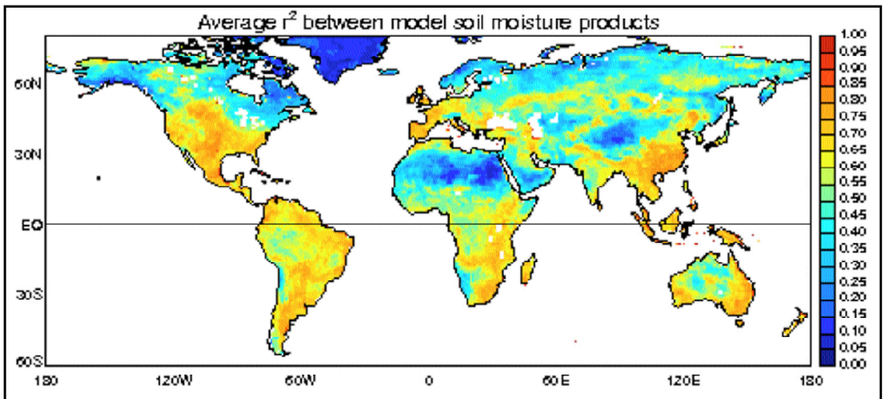

Figure 1. Average r^2 between land surface model (LSM) root zone soil moisture time series, for LSMs driven with the same meteorological forcing. (At a given location, an r^2 value was computed for each pairing of LSMs in the study; the average of the r^2 values is plotted.) The plotted values show the degree to which the LSM products from the different models contain the same information on the time variability of soil moisture (from Koster et al. 2008).

nisms that maintain drought across the seasonal cycle and from one year to the next? What is the role of the different ocean basins, including the impact of El Nino/Southern Oscillation (ENSO), the Pacific Decadal Oscillation (PDO), the Atlantic Multi-decadal Oscillation (AMO), and warming trends in the global oceans? What is the role of the land? To what extent can droughts develop independently of ocean variability due to year-to-year memory that may be inherent to the land?

A number of groups contributed model runs to the project. NASA's Global Modeling and Assimilation Office (GMAO) contributed runs made with version 1 of the NASA Seasonal-to-Interannual Prediction Project (NSIPP-1) AGCM. NOAA's Climate Prediction Center, with support from the Climate Test Bed, contributed runs made with the Global Forecast System (GFS) AGCM. NOAA's Geophysical Fluid Dynamics Laboratory (GFDL) contributed runs made with the AM2 AGCM, while the Lamont-Doherty Earth Observatory of Columbia University contributed runs made with the NCAR CCM3.0 AGCM. NCAR contributed runs made with the CAM3.5 AGCM. An additional set of runs was made by COLA/University of Miami with the coupled (atmosphere-ocean) CCSM3.0 model employing a novel adjustment technique to nudge the coupled model towards the imposed SST forcing patterns.

While the full set of experiments covers a wide range of SST forcing patterns and includes runs that examine the impact of land-atmosphere feedbacks, the baseline set of experiments examine drought response to the three leading patterns of annual mean SST variability. These consist of a global trend pattern, a Pacific ENSO-like pattern, and an Atlantic pattern that resembles the Atlantic Multi-decadal Oscillation (AMO). Figure 2 shows, for example, the results from all 8 combinations (warm and cold phases) of the Pacific and Atlantic patterns for the 5 AGCMs. A key result is that all the models agree that the combination of a cold Pacific and warm Atlantic (PcAw) tends to produces the largest precipitation deficits, while the combination of a warm Pacific and cold Atlantic (PwAc) tends to produce the largest precipitation surpluses.

The various experiments and information on access to the output from the various model runs may be found at: ftp://gmaoftp.gsfc.nasa.gov/pub/data/clivar_drought_wg/README/www/index.html

References

Dirmeyer, P. A., X. Gao, M. Zhao, Z. Guo, T. Oki and N. Hanasaki, 2006: The Second Global Soil Wetness Project (GSWP-2): Multi-model analysis and implications for our perception of the land surface. Bull. Amer. Meteor. Soc., 87, 1381-1397.

Gutzler, D. and S. Schubert: The U.S. CLIVAR Working Group on Long-Term Drought," U.S. CLIVAR Variations (Spring 2007, volume 5, No. 1).

Koster, R. D., Z. Guo, R. Yang, P. A. Dirmeyer, and K. Mitchell, 2008: On the Nature of Soil Moisture in Land Surface Models. Submitted to J. Climate.

Schubert, S. and the extended USCLIVAR drought working group, 2009: A USCLIVAR Project to Assess and Compare the Responses of Global Climate Models to Drought-Related SST Forcing Patterns: Overview and Results. To be submitted to J. Climate .

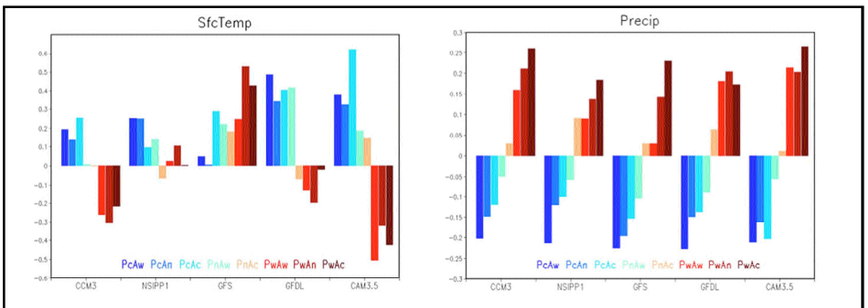

Figure 2. The annual and continental United States mean responses for a) precipitation and b) surface temperature for all 8 combinations of the Pacific and Atlantic SST forcing patterns, for all 5 participating AGCMs. The colors refer to the forcing patterns consisting of combinations of the Pacific (ENSO-like) and Atlantic (resembling the AMO) SST patterns. For example, PcAw indicates an SST forcing consisting of the cold phase of the Pacific pattern and the warm phase of the Atlantic, while PcAn indicates the cold phase of the Pacific pattern and the neutral phase of the Atlantic pattern (climatological SSTs).

Analysis of the multi-model U.S. CLIVAR Drought Working Group simulations

Philip J. Pegion and Arun Kumar

The U.S. CLIVAR Drought working group formed in December 2006. Some of the goals of the working group were to coordinate evaluations of existing model simulations, and to also coordinate new experiments designed to address some of the outstanding uncertainties related to drought variability and predictability. Six modeling groups joined in the effort and produced a wealth of model simulation data that will be analyzed for many years. The primary goal of model experiments was to quantify the role sea surface temperature (SST) variability on changes to the atmospheric circulation that lead to drought.

The six modeling groups were NASA-GSFC, LDEO, GFDL, UMD/NCAR, UM/COLA, NCEP/CPC. Five of the groups, with the exception of UM/COLA preformed the experiments with a global atmospheric general circulation model (AGCM) forced with the identical SSTs. UM/COLA did the experiments with a coupled model. The models were the NSIPP1 AGCM (Bacmeister et al. 2000, Schubert et al. 2004), CCM3 (Kiehl et al. 1998, Seager et al. 2005), GFDL AM2.1 (Delwoth e al 2006, The GFDL Model Development Team 2004, Milly and Shmakin 2002), CAM3.5, and the GFS (Campana and Caplan 2005). These five models have diverse developments histories, and comprise of both spectral and grid-point models, different physical parameterizations and spatial resolutions.

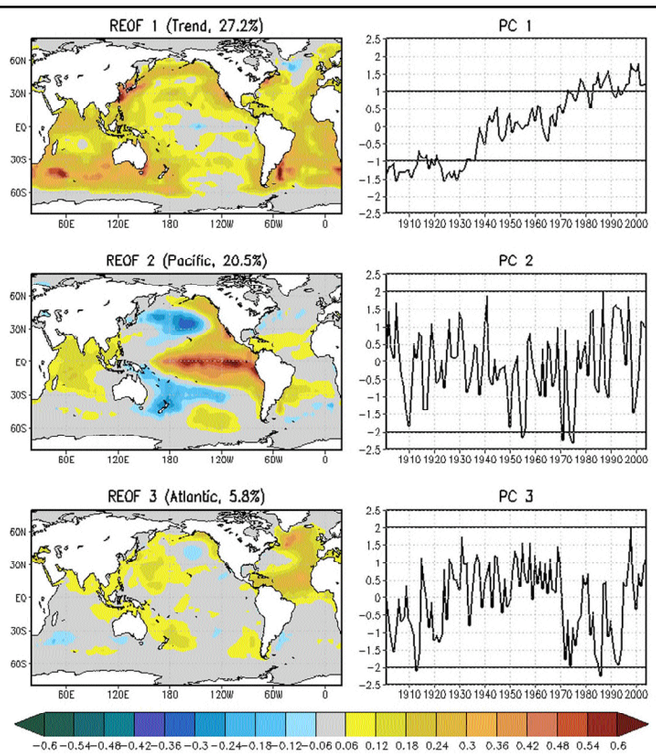

Figure 1. The three leading rotated EOFs of HADISST annual mean SST for 1901-2004. Combined these three EOFs explain over 52% of the inter-annual variance.

The AGCM's were forced with a set of idealized anomalous SST forcing. The SST anomalies were produced from a rotated empirical orthogonal function (REOF) analysis of the annual mean HADISST (Rayner et al. 2003) for the years 1901-2004, these three leading REOFs together explain over half of the inter-annual variance. The loading patterns and principal components are shown in Fig. 1. The three patterns are referred to as the Trend, Pacific, and North Atlantic patterns. The purpose of the idealized experiments was to isolate the influence of each pattern separately as due to the short historical record of SST observations, it is difficult to isolate the impact of each SST mode in AMIP type simulations or in observations.

The sets of experiments consisted of each AGCM run with a repeating seasonal cycle of climatological SSTs, and also with fixed anomalies added to the repeating seasonal cycle. To assess the role each of SST patterns has on climate variability, the patterns are scaled by +/- the standard deviation of the principal component. The trend is scaled by 1 standard deviation, which roughly represents a period of 1901-1942 for the negative scaling, and 1965-2004 for the positive period. The other EOFs are scaled by twice the standard deviation to emphasize their atmospheric influence. The anomaly patterns are then added to a repeating climatological seasonal cycle of the HADISST data, with the climatology based on the 1901-1999 period. The treatment of sea-ice was left to the individual modeling groups, but an ice extent climatology was specified. To isolate the role of each of the SST patterns, the anomalies for the Pacific pattern were set to zero in the Atlantic Basin, and conversely, the anomalies in the Pacific and Indian oceans were set to zero in the North Atlantic forcing pattern.

Each modeling center ran many long simulations with the idealized SST pat-

terns, and a control run with the climatological SSTs. The runs varied between 36 years (NCEP GFS) to 51 years for the other models with the first year discarded as spin-up. Both the positive and negative polarity of each pattern was used to force the AGCM. In addition, various combinations of these patterns were used in additional experiments. In total, there were 15 different experiments run with the SST patterns. The results presented in this paper are for the model response to each of the individual SST patterns, and does not address how the atmospheric response to the SST patterns interplay with each other, or the relative role of the tropical vs. extra-tropical SSTs.

This analysis looks at agreement between models responses the different SST forcing patterns; as such an agreement enhances our confidence in AGCM based results. The response is defined as the multi-model mean of the positive polarity minus the negative polarity experiments. The annual mean response in temperature and precipitation for the 3 leading patterns is shown in Fig. 2. Shading indicates model agreement, on the sign of the anomalous response. The precipitation response to the trend SST patterns is mainly confined over the ocean, and coastal regions. The response includes an increase in precipitation over the southern tip of Indian, extending eastward through the maritime continent, with a decrease of precipitation over the central equatorial pacific. There is also an increase in precipitation over Central America and a warming over most of the globe.

The Pacific SST pattern shows a more robust response, with increased precipitation over most of the equatorial Pacific, a decrease over the maritime continent. There is also a decrease in precipitation over the Amazon and extending across the tropical Atlantic Ocean into Africa, and an increase in precipitation over North America and the southern portion of South America. The temperature response shows warming over the tropical land masses and over northwestern Canada into Alaska, and a cooling over the central United States.

The precipitation response to the North Atlantic SST pattern shows an increase over the regions of positive SST anomalies, and reduced precipitation for most of the globe, with the exception over the Indonesian region. The surface temperature response is a large scale warming that extends across northern Africa and into southern Asia. There is also a signal of increased surface temperature over the southern Great Plains, and Mexico, and central South America.

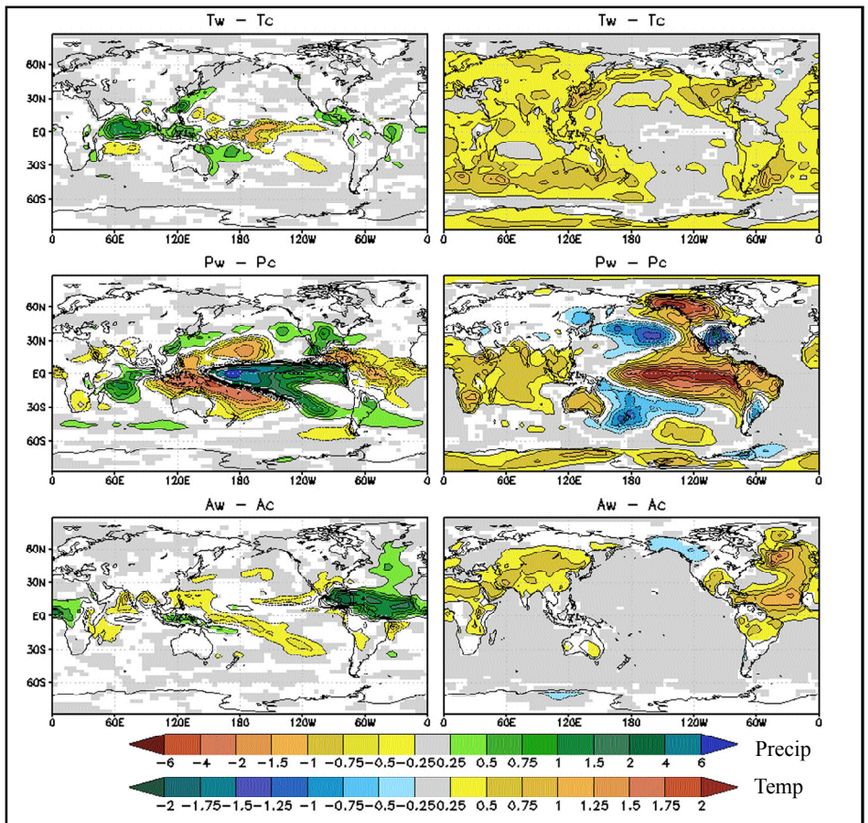

Figure 2. The multi-model response to the three patterns, precipitation (left) and surface temperature (right). Contours show the model mean response, and shading indicated where at least 4 out of the 5 models (3 out of 4 for the Trend patterns, as CCM3.5 did not complete a negative Trend experiment) produced the same sign response. Units are mm/day for precipitation and ^{O}K for temperature.

The impact of SST patterns over the United States is dominated by the Pacific SST pattern, but upon closer inspection, the precipitation response to the Trend and Atlantic SST forcing are also statically significant at the 5% level when average over United States Great Plains, which is defined by the region within 30^{O}N to 50^{O}N, and 95^{O}W to 105^{O}W. The probability density function (PDF) of annual mean precipitation anomalies for the Great Plains is shown in Fig. 3. Although the mean precipitation response to the Trend is fairly small (0.04 mm/day), it does have a role in shifting the odds of having long term droughts. As a comparison, the Dust Bowl's precipitation anomalies over the US great plains average for the years 1932-1938 was only -0.2mm/day based on GHCN gridded precipitation data. The PDFs for the Atlantic and Pacific SST experiments have greater separation.

In order to quantify the change in the odds of having long term drought, all of the models were pooled together and resampled to calculate the odds of having 3-years with below normal precipitation

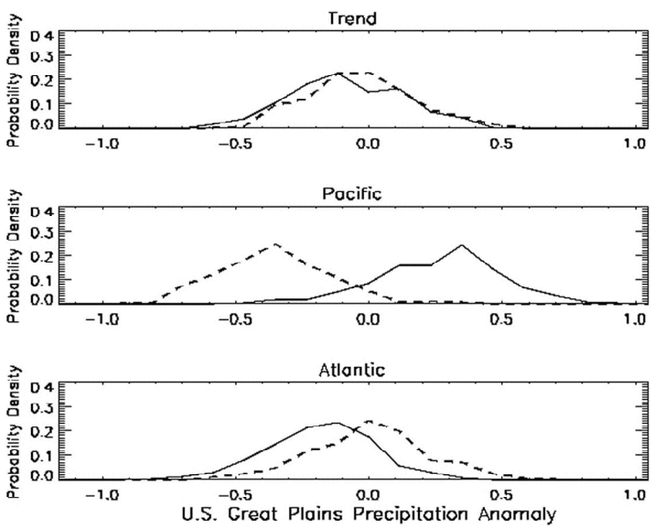

Figure 3. Probability density function of annual mean precipitation over the US Great Plains (95W-105W, 30N-50N) for all of the models combined (235 years of simulation for the Trend forcing (top) and Pacific forcing (middle), and 185 years for the Atlanticpattern (bottom). Solid curve is from the warm (positive) forcing, and the dashed is for the negative pattern. Units are mm/day.

in a row. The odds were calculated randomly selecting 3 years of precipitation with replacement, and counting how many times the sample contained all 3 years of negative precipitation anomalies. The re-sampling was done 10,000 times for each pattern. If a distribution is normally distributed, the expected probability for 3-years in a row of below normal precipitation is 12.5%. The Monte Carlo estimate for the warm Pacific pattern shows only a 0.1 % chance of having 3 years in a row of below average precipitation, compared to 79% when the Pacific is cool. The Atlantic forces a shift in probability from 36.7% chance of having 3 dry years in the warm phase versus a 3.9% chance when it is cool. The Trend shifts the chance to 24.0% for the warm pattern compared to 7.0% when the SSTs were cool. The climatology runs for all of the models pooled together give a chance of 13.7 percent chance of having 3 dry years. The deviation from 12.5% is due to the skewness of precipitation.

Because these experiments were done with many different AGCMs, more confidence can be put in the results, with the caveat that these are all AGCMs with are just responding to SST anomalies and the possible influence of coupled air-sea interaction is ignored. That being said, we have shown that the Pacific pattern is the dominant forcing on precipitation variability globally, which is not surprising since that pattern also has the largest amplitude. The Atlantic and Trend SST anomalies do also produce significant changes in precipitation, just more localized, but the temperature response to the Atlantic and Trend does have worldwide impacts.

Acknowledgement

This work was carried out as part of a U.S. CLIVAR drought working group activity supported by NASA, NOAA, and NSF to coordinate and compare climate model simulations forced with a common set of idealized SST patterns. The authors would like to thank NASA's Global Modeling and Assimilation Office (GMAO) for making the NSIPP1 runs available, the Lamont-Doherty Earth Observatory of Columbia University for making their CCM3 runs available, NOAA's Climate Prediction Center (CPC)/Climate Test Bed (CTB) for making the GFS runs available, NOAA's Geophysical Fluid Dynamics Laboratory (GFDL) for making the AM2.1 runs available, the National Center for Atmospheric Research (NCAR) for making the CAM3.5 runs available, and the Center for Ocean Land Atmosphere (COLA) and the University of Miami's Rosenstiel School of Marine and Atmospheric Science for making the CCSM3.0 coupled model runs available.

References

Bacmeister J., P. J. Pegion, S. D. Schubert, and M. J. Suarez, 2000: An atlas of seasonal means simulated by the NSIPP 1 atmospheric GCM. Vol. 17. NASA Tech. Memo. 104606, Goddard Space Flight Center, Greenbelt, MD, 194 pp.

Campana, K. and P. Caplan, Editors, 2005: Technical Procedure Bulletin for T382 Global Forecast System (http://www.emc.ncep.noaa.gov/gc_wmb/Documentation/TPBoct05/T382.TPB.FINAL.htm).

Delworth et al., 2006. GFDL's CM2 global coupled climate models - Part 1: Formulation and simulation characteristics, J. Climate, 19, 643-674.

The GFDL Global Atmospheric Model Development Team, 2004. The New GFDL Global Atmosphere and Land Model AM2-LM2: Evaluation with Prescribed SST Simulations. J. Climate, 17, 4641-4673.

Kiehl, J.T., J.J. Hack, G. Bonan, B.A. Boville, D. Williamson and P. Rasch, 1998. The National Center for Atmospheric Research Community Climate Model: CCM3. J. Climate, 11, 1131-1149.

Milly, P. C. D., and A. B. Shmakin, 2002. Global modeling of land water and energy balances. Part I: The land dynamics (LaD) model. J. Hydrometeorology, 3, 283-299.

Rayner, N. A., D. E. Parker, E. B. Horton, C. K. Folland, L. V. Alexander, D. P. Rowell, E. C. Kent, and A. Kaplan, 2003: Global analyses of sea surface temperature, sea ice, and night marine air temperature since the late nineteenth century, J. Geophys. Res., 108(D14), 4407.

Schubert, S.D. M.J. Suarez, P.J. Pegion, R. D. Koster, and J.T. Bacmeister, 2004: Causes of long-term drought in the U.S. Great Plains,. J. Climate, 17, 485-503.

Seager, R., Y. Kushnir, C. Herweijer, N. Naik and J. Velez, 2005: Modeling tropical forcing of persistent droughts and pluvials: 1856-2000. J. Climate, 18, 4068-4091. ■

VARIATIONS

The Caribbean Low-Level Jet: Regional Dynamics and its Relationship to Precipitations

Kerry H. Cook and Edward K. Vizy
Department of Geological Sciences and Institute for Geophysics
Jackson School of Geosciences
The University of Texas at Austin

The Caribbean low-level jet (CLLJ) is an easterly jet located over the Caribbean Sea off the northern coast of South America, south of Hispaniola (Haiti and the Dominican Republic). It is present throughout the year and transports large amounts of moisture, forming a primary connection between the Gulf of Mexico and the tropical Atlantic Ocean. For most of the year the jet core is located very close to the surface, at 925 hPa, but in the fall the jet core lifts higher, up to 800 hPa in September and October.

The CLLJ is depicted near the edge of the North American Regional Reanalysis (NARR; Mesinger et al. 2006) domain (Fig. 1), providing an opportunity for a high-resolution (32 km x 32 km) investigation of the regional dynamics and, since precipitation is assimilated in the NARR, an analysis of the relationship between the CLLJ and rainfall over the central U.S, Mexico, Central America, and the Caribbean. Note that, at 925 hPa, the highest wind speeds in the NARR domain are those of the CLLJ.

Dynamics of the CLLJ: Seasonality

The CLLJ is present all year, with a peak monthly-mean magnitude in July of about 12 m/s. The jet is also strong in December at January, with wind speeds of 8-9 m/s. Minima of 6-8 m/s occur in May and October. This semiannual seasonal cycle is in contrast to that of the climatological Great Plains low-level jet (GPLLJ), which forms only in boreal summer (if one takes a wind speed of 3 m/s as the threshold velocity to define a "jet"). Muñoz et al. (2008) relate seasonality in the magnitude of the CLLJ to a similar semiannual cycling of the magnitude of the meridional SLP and temperature gradients in the NARR, explaining that the CLLJ is, to first order, geostrophic between 925 and 800 hPa. The u-momentum balance is not at all geostrophic, with advection and friction similar in magnitude to Coriolis and pressure gradient accelerations.

A complete analysis of the horizontal momentum balance confirms that the seasonal cycle of the CLLJ is primarily due to seasonal variations in the positive meridional geopotential height gradient between far northern South America and the central Caribbean. In boreal summer, this gradient is strong because of the position of the North Atlantic subtropical high (NASH) to the north of the CLLJ. The secondary jet speed maximum in boreal winter occurs because low geopotential heights develop to the south as part of the South America monsoon system, and this also generates strong positive meridional gradients across the CLLJ region. Minima in the CLLJ magnitude in the transition seasons reflect the absence of these enhancements to the positive meridional gradient that is nonetheless present and relatively strong all year as the tropical easterly flow funnels between the north coast of South America and the islands of the Greater Antilles (Cuba, Puerto Rico, Jamaica, and Hispaniola).

here is a distinct difference in the large-scale context of the CLLJ between the summer and winter seasons. During the months of October through April, the jet flow continues westward over the Caribbean Sea, finally obtaining a southward component in meeting the orography of Central America and entering the eastern Pacific basin. In contrast, during the months of May through September, the CLLJ splits into two branches over the central Caribbean Sea. One branch proceeds westward and enters the Pacific basin while the northern branch flows northward connecting the CLLJ with moisture transport throughout the Caribbean and Gulf of Mexico, and with the climatological GPLLJ and water vapor transport into the central U.S. Differences between these two states, shown in Figure 2, indicates that the difference in the circulation essentially amounts to a northerly wind anomaly that is related to the development of positive zonal height gradients associated with summer heating over Central America and southern Mexico.

Dynamics of the CLLJ: Diurnal Variations

Unlike the climatological GPLLJ, which is composed primarily of individual low-level jet events that develop over the central U.S. at night in the summer months, the diurnal cycle of the CLLJ is not very dramatic. There are two wind speed minima during each 24 hour peri-

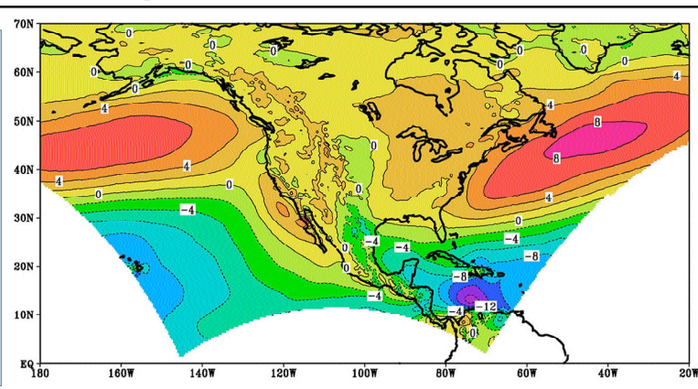

Figure 1. Zonal wind speed at 925 hPa in July over the NARR domain for the 1979-2007 climatology. Contour interval is 2 m/s.

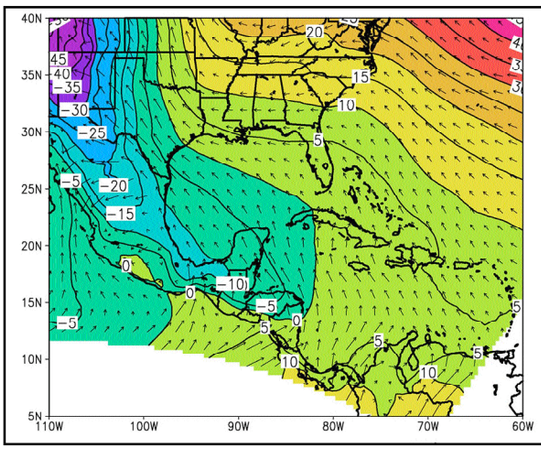

Figure 2. Differences in 925 hPa geopotential heights (contour interval is 5 gpm) and winds (vector scale is in m s-1) between the May – September and October – April averages for 1979-2007 from the NARR. Shading denotes negative geopotential height differences.

od throughout the year, at about 4 AM and at 4 PM. A progressive weakening of the jet through the afternoon is more pronounced than the nighttime weakening, so the 4 PM minimum is more distinct. This afternoon minimum is explained by considering meridional accelerations, which couple to the zonal flow through Coriolis accelerations. The meridional acceleration is southward during the day and northward at night, and one cause of this diurnal sign change is variations in the meridional height gradient which strengthens from 4 AM to 4 PM, and weakens from 4 PM to 4 AM. This is caused by the diurnal cycle of heating over northern South America. The center of the daytime heating is over the northern Andes, presumably in association with sensible heating over the elevated surface. So the meridional wind variation is a land/sea breeze (solenoidal circulation), with anomalous southward acceleration during the day and anomalous northward flow at night, and this contributes to the weak diurnal variation of the CLLJ.

Relationship of the CLLJ to Precipitation: A Drought Connection?

Magaña et al. (1999) relate seasonal changes in the CLLJ to the occurrence of the so-called "midsummer drought", which is a normal feature of the southern Mexico and Central America seasonal cycle defined by lower rainfall rates in July and August as compared with June and September/October. Even though this feature is not a drought in the sense of being an anomalous or extreme event, the fact that the CLLJ and rainfall are related on sub-seasonal time scales suggests that interannual rainfall variations – including, perhaps, the occurrence of drought in the central U.S., Central America, and Mexico – may be associated with CLLJ variations.

wo approaches were taken to understand if there is a relationship between the CLLJ and drought. One was to ask if the CLLJ tends to be anomalous during times of drought (e.g., individual dry years). For the time period covered by the NARR climatology (1979-2006), three summers emerge as exceptionally dry in the central U.S (100-90°W and 30-50°N), namely, 1980, 1988, and 2007, consistent with other data sets and studies. The average CLLJ for these three drought years is relatively weak, especially in June and August. But an examination of the individual years shows that the jet was only weak in 1988, and this dominates the small-sample-size composite. There is no consistent signal among the 3 years.

ver Central America and southern Mexico (100-80°W and 10-20°N), only one year (2003) is identifiable as a drought year in the NARR period. Since the purpose of this study is to understand the CLLJ's relationship to drought in a general, climatological sense, this approach was abandoned. Instead, a second approach was pursued in which we focus on times with strong and weak CLLJs, and ask if and where precipitation is anomalous at the same time.

To explore connections between the strength of the CLLJ and regional rainfall within the NARR domain we first define a CLLJ index as the magnitude of the monthly-mean 925 hPa wind speed in an area bounded by 75-70°W and 12-15°N, and standard deviations from the 1979-2007 monthly mean zonal wind speed are calculated. Strong and weak CLLJ months are selected based on these standard deviations, requiring that a strong jet exceeds the mean by one standard deviation and that a weak jet is at least one standard deviation below the mean. Of the 348 months (29 years) analyzed, 16% (58 months) are identified as strong CLLJ months, and 14% (50 months) as weak CLLJ months. The distribution skews a bit toward strong CLLJ events because of an apparent trend after 2000. Correlations between the standard deviations of the CLLJ index and rainfall were calculated over the NARR time period (not shown) and composite rainfall distributions for strong and weak CLLJ months were assembled. Conclusions draw from these two analyses, presented below, are consistent.

To increase the numbers of events composited and focus on differences between the two states of the CLLJ-related flow, results are presented for the summer (MJJAS), when the CLLJ has a northward component, and for the rest of the year (the ONDJFMA mean) when it flows to the west. This places 24 monthly-mean events in the "strong CLLJ" composite and 25 in the "weak CCLJ" composite.

Figure 3a displays contours of the MJJAS mean precipitation (mm day-1) and the vertically-integrated water vapor transport (?105 kg m-1) from the NARR climatology. Falsely low rainfall rates, for example over Cuba, Hispaniola, and along the Texas/Mexico border, are related to either a lack of reported rainfall observations or the transition from the dense observing network over the U.S. From a visual examination of the vertically-integrated moisture flux climatology in Fig. 3a it appears that the northward branch of the CLLJ and the GPLLJ are part of the same system (see also Mestas-Nuñez et al. 2007), suggesting that they may vary in concert. But the moisture transport and precipitation anomalies from the composites of strong and weak CLLJ events (Figs. 3b and c, respectively) show clearly that the north-

ward flow across the Gulf of Mexico is not enhanced (diminished) when the CLLJ is strong (weak) during the summer months. Instead, strong (weak) CLLJ wind speeds are associated with enhanced (reduced) moisture transport into the Caribbean from the northeast, high (low) rainfall rates over Hispaniola, and strong (weak) easterly moisture advection across the western Caribbean. The resulting moisture divergence anomalies over the central and western Caribbean are associated with negative (positive) rainfall anomalies in the strong (weak) CLLJ case. Note that there is no evidence of a dipole pattern of precipitation anomalies between the Atlantic warm pool and the central U.S. (e.g., as suggested by Wang 2007) when the CLLJ is used as a selector.

According to the NARR, rainfall rates are enhanced off the east and west coasts of Panama and Costa Rica and reduced over land when the CLLJ is strong. It is not exactly clear how or if this signal is related to the findings of Magaña et al. (1999), who suggest that a strong CLLJ is associated with high orographic rainfall in eastern Panama and Costa Rica and drying to the west due to a rainshadow effect. We examined the response as in Figs. 3b and c at high resolution, taking advantage of NARR's 32 grid spacing, and did not find rainfall enhancement over land that would indicate the orographic mechanism/rainshadow effect. However, the rainfall assimilated into the NARR in these regions has a coarser resolution than the grid onto which it is interpolated, so perhaps the relationship emerges when station data is used.

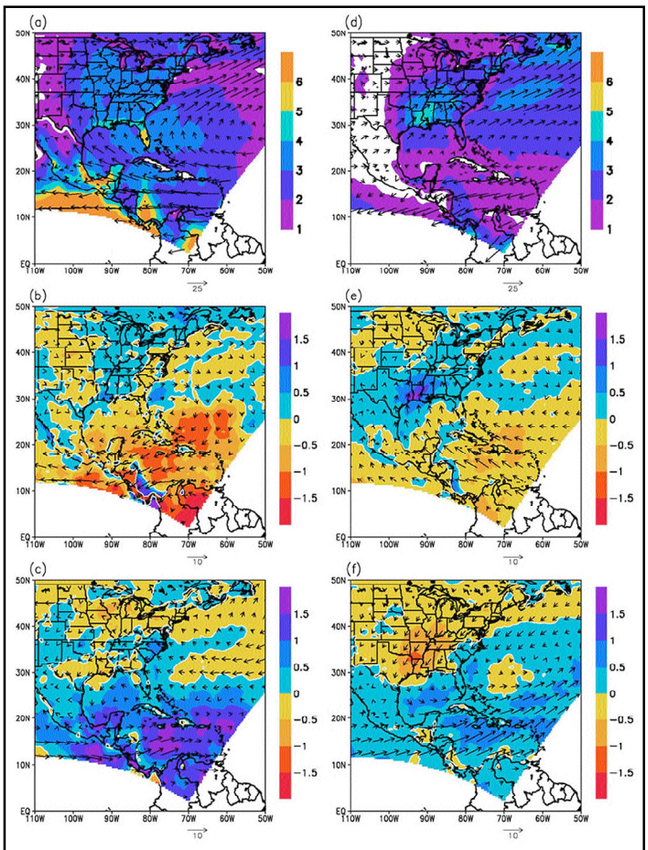

Figure 3. May – September (a) climatological mean precipitation (mm day-1) and vertically integrated water vapor transport (?105 kg m-1), and (b) strong and (c) weak Caribbean low-level jet composite minus climatological mean precipitation and vertically integrated water vapor transport difference. Additionally, October – April (d) climatological mean precipitation and vertically integrated water vapor transport, and (e) strong and (f) weak Caribbean low-level jet composite minus climatological mean precipitation and vertically integrated water vapor transport difference.

Figure 3d displays contours of the ONDJFMA mean precipitation (mm day-1) and the vertically-integrated water vapor transport (?105 kg m-1) from the NARR climatology. In contrast to the MJJAS climatology (Fig. 3a), there is no evident connection between the CLLJ and the transport of moisture into the central U.S. and Mexico during these months. But when strong CLLJ events are composited, as seen in Fig. 3e, it is clear that a strong CLLJ during these non-summer months is accompanied by the formation of a meridional CLLJ branch that is similar to the summer climatological pattern (Fig. 3a). During these strong jet events, moisture is transported across the Gulf of Mexico and into the southern Great Plains and the southeastern U.S. Positive rainfall anomalies centered in Louisiana and Texas occur as a result. When the ONDJFMA CCLJ is weak (Fig. 3f), there is southwestward anomalous moisture transport across the southern Great Plains and low rainfall.

Closing Remarks

Despite the apparent relationship between the CLLJ and the GPLLJ, we found no systematic connection between variations in the CLLJ and summer drought in the Great Plains in examining the NARR for 1979-2007. However, the most extreme dry year of the period for the central U.S. was 1988, and the CLLJ was quite weak that year so a case-study approach might be useful for uncovering a drought mechanism relevant to other time periods, past or future. Further work on the non-summer months would also be useful, for example, for fall and early spring in isolation to understand the dynamics of seasonal transitions that may be informative about the dynamics of how drought periods begin and are broken.

References

Magaña, V., J.A. Amador, and S. Medina, 1999: The midsummer drought over Mexico and Central America. J. Climate, 12, 1577-1588.

Mesinger, F., and Coauthors, 2006: North American regional reanalysis. Bull. Amer. Meteor. Soc., 87, 343-360.

Mestas-Nuñez, A.M., D.B. Enfield, and C. Zhang, 2007: Water vapor fluxes over the intra-America sea: Seasonal and interannual variability and associations with rainfall. J. Climate, 20, 1910-1922.

Muñoz, E., A. Busalacchi, S. Nigam, and A. Ruiz-Barradas. 2008: Winter and summer structure of the Caribbean low-level jet. J. Climate, 21, 1260-1276.

Wang, C., 2007: Variability of the Caribbean low-level jet and its relations to climate. Climate Dynamics, 29, 411-422.

U.S. CLIVAR

Calendar of CLIVAR and CLIVAR-related meetings

Further details are available on the U.S. CLIVAR and International CLIVAR web sites: www.usclivar.org and www.clivar.org

89th AMS Annual Meeting
11-15 January 2009
Phoenix, Arizona
Attendance: Open
Contact: http://www.ametsoc.org

U.S. CLIVAR Western Boundary Current Workshop
15-17 January 2009
Phoenix, Arizona
Attendance: Open
Contact:
http://www.usclivar.org/WBCWorkshop2009.php

CLIVAR Working Group on Seasonal to Interannual Prediction
12-14 January 2009
Miami, Florida
Attendance: Invited
Contact: http://www.clivar.org

AMMA-Ocean/TACE/PIRATA meeting
2-6 February 2009
Toulouse, France
Attendance: Limited
Contact: http://amma-international.org

Ninth International Conference on Southern Hemisphere Meteorology and Oceanography
9-13 February 2009
Melbourne, Australia
Attendance: Open
Contact: http://9icshmo.org

NOAA Climate Predictions Applications Workshop
24-27 March 2009
Norman, Oklahoma
Attendance: Open
Contact: http://climate.ok.gov/cpasw/

Workshop on El Nino and Climate Change
25-26 March 2009
Perth, Australia
Attendance: Open
Contact: http://www.greenhouse2009.com

CLIVAR Pacific Implementation Panel Meeting
27-28 March 2009
Perth, Australia
Attendance: Invited
Contact: http://www.clivar.org

3rd ARGO Science Meeting - The Future of ARGO
25-27 March 2009
Hangzhou, China
Attendance: Open
Contact:
http://www.argo.ucsd.edu/ASW3.html

WCRP Joint Scientific Committee Meeting
6-9 April 2009
College Park, Maryland
Attendance: Invited
Contact: http://www.clivar.org

European Geophysics Union General Assembly
19-24 April 2009
Vienna, Austria
Attendance: Open
Contact: http://www.egu.org

CLIVAR Working Group on Ocean Modeling: Panel Meeting
30 April - 1 May 2009
Exeter, UK
Attendance: Invited
Contact: http://www.clivar.org

CLIVAR Working Group on Ocean Modeling: Mesoscale Eddies Workshop
27-29 April 2009
Exeter, UK
Attendance: Open
Contact:
http://www.metoffice.gov.uk/conference/mesoscale_workshop/

1st US Atlantic Meridional Overturning Circulation Meeting
4-6 May 2009
Annapolis, Maryland
Attendance: Open
Contact:
http://www.AtlanticMOC.org/AMOC2009.php

World Ocean Conference
11- 15 May 2009
Manado, Indonesia
Attendance:Open
Contact:
http://www.woc2009.org/home.php

NASA Ocean Vector Wind Science Team Meeting
18-20 May 2009
Woods Hole, MA
Attendance: Invited
Contact: http://coaps.fsu.edu/scatterometry/meeting/

CLIVAR/GOOS Indian Ocean Panel
3-5 June 2009
Le Reunion, France
Attendance: Invited
Contact: http://www.clivar.org

U.S. CLIVAR OFFICE
1717 Pennsylvania Avenue, NW
Suite 250
Washington, DC 20006

Subscription requests, and changes of address should be sent to the attention of the U.S. CLIVAR Office (cstephens@usclivar.org)

U.S. CLIVAR contributes to the CLIVAR Program and is a member of the World Climate Research Programme